Rose bengal in poly(2-hydroxyethyl methacrylate) thin films: self-quenching by photoactive energy traps

2017 Methods Appl. Fluoresc. 5 014010

(http://iopscience.iop.org/2050-6120/5/1/014010)

Methods and Applications in Fluorescence

RECEIVED
4 November 2016

REVISED
1 February 2017

ACCEPTED FOR PUBLICATION
21 February 2017

PUBLISHED
8 March 2017

PAPER

Rose bengal in poly(2-hydroxyethyl methacrylate) thin films: self-quenching by photoactive energy traps

Sergio D Ezquerra Riega[1], **Hernán B Rodríguez**[1,2,3] **and Enrique San Román**[1,3]

[1] CONICET—Universidad de Buenos Aires, Instituto de Química Física de los Materiales, Medio Ambiente y Energía (INQUIMAE), Ciudad Universitaria, Pab. II, Buenos Aires, Argentina
[2] INIFTA (UNLP-CONICET), Facultad de Ciencias Exactas, Universidad Nacional de La Plata, Diag. 113 y Calle 64, La Plata, Argentina
[3] Authors to whom any correspondence should be addressed.

E-mail: esr@qi.fcen.uba.ar **and** hernanrodriguez@inifta.unlp.edu.ar

Keywords: rose bengal, polymer films, pHEMA, energy trapping, fluorescence, singlet molecular oxygen

Supplementary material for this article is available online

Abstract

The effect of dye concentration on the fluorescence, Φ_F, and singlet molecular oxygen, Φ_Δ, quantum yields of rose bengal loaded poly(2-hydroxyethyl methacrylate) thin films (~200 nm thick) was investigated, with the aim of understanding the effect of molecular interactions on the photophysical properties of dyes in crowded constrained environments. Films were characterized by absorption and fluorescence spectroscopy, singlet molecular oxygen ($^1O_2$) production was quantified using a chemical monitor, and the triplet decay was determined by laser flash-photolysis. For the monomeric dilute dye, $\Phi_F = 0.05 \pm 0.01$ and $\Phi_\Delta = 0.76 \pm 0.14$. The effect of humidity and the photostability of the dye were also investigated. Spectral changes in absorption and fluorescence in excess of 0.05 M and concentration self-quenching after 0.01 M are interpreted in the context of a quenching radius model. Calculations of energy migration and trapping rates were performed assuming random distribution of the dye. Best fits of fluorescence quantum yields with concentration are obtained in the whole concentration range with a quenching radius $r_Q = 1.5$ nm, in the order of molecular dimensions. Agreement is obtained only if dimeric traps are considered photoactive, with an observed fluorescence quantum yield ratio $\Phi_{F,trap}/\Phi_{F,monomer} \approx 0.35$. Fluorescent traps are capable of yielding triplet states and $^1O_2$. Results show that the excited state generation efficiency, calculated as the product between the absorption factor and the fluorescence quantum yield, is maximized at around 0.15 M, a very high concentration for random dye distributions. Relevant information for the design of photoactive dyed coatings is provided.

Abbreviations

RB	rose bengal
pHEMA	poly(2-hydroxyethyl methacrylate)
DCM	dichloromethane
DPBF	1,3-diphenylisobenzofuran
DT	dark traps
BDT	bright dimeric traps
LAF	Loring–Andersen–Fayer
LFP	laser flash photolysis
MB	methylene blue

1. Introduction

Rose bengal (RB) has long since been considered a prototypical photosensitizer for the generation of singlet molecular oxygen, $^1O_2$, with $\Phi_\Delta = 0.76$ in water and ethanol in its dianionic form [1]. It is also a weak fluorophore, with $\Phi_F = 0.018$ and 0.11 in water and methanol, respectively [2], and 0.13 when immobilized into cellulose beads, where the triplet quantum yield amounts to $\Phi_T = 0.57$ [3]. Neckers claimed that, on attaching chemically RB to a polystyrene-divinylbenzene copolymer at high concentrations, Φ_Δ values as high as 0.91 were obtained [4]. However, these particularly high values are difficult to understand and

contradict the common knowledge that organic dyes undergo self-quenching when interactions are forced on increasing concentration.

Certain molecules tend to increase their fluorescence quantum yield when immobilized at low concentrations into rigid polymers. As an example, a fluorescein derivative, 9-[1-(2-Methyl-4-methoxyphenyl)]-6-hydroxy-3H-xanthen-3-one, shows in neutral form an increase of nearly 30 times in Φ_F from its value in solution when included into microcrystalline cellulose [5]. A possible reason is the hindrance of formation of a TICT state involving rotation of the dye phenyl group. However, at high concentrations, organic dyes are known to interact through π stacking, leading to aggregation induced excited state quenching. For that reason, encapsulation of dyes inside polymer nanoparticles is generally performed at rather low dye loadings, usually less than 0.5 wt%, when they are used for bioimaging or other applications requiring high brightness [6]. In spite of this fact, in certain cases distorted H-aggregate formation leads to dimer fluorescence. This is probably the case of RB, which was found to build up fluorescent dimers when entrapped into microcrystalline cellulose [7], for which $\Phi_F = 0.07$, 60% of the value found for the monomeric dye in the cellulose environment. Remarkably, for the monomer Φ_F is similar to the value found in methanol [2].

We investigated recently the effect of dye concentration on the photosensitizing properties of phloxine B (PhB) included into poly(2-hydroxyethyl methacrylate) (pHEMA), a polymer that forms hydrogels in water and, upon crosslinking, builds up stable materials, mainly used in the production of contact lenses [8]. It was demonstrated that the ability of PhB included in pHEMA to sensitize the formation of $^1O_2$, which parallels fluorescence emission, reaches its maximum at a dye concentration around 2 wt% (~0.03 M). Indeed, the product between the absorption factor and Φ_F shows a bell-shaped behavior peaking at this concentration, which is determined by the quenching radius, i.e., the minimum distance at which two dye molecules may be located avoiding self-quenching. Film thickness is also relevant, as only those $^1O_2$ molecules located at a distance below the diffusion length can reach the film surface. As PhB has a low Φ_Δ value, results were considered as a proof of concept for the development of heterogeneous photosensitizers, mainly photoactive coatings with antimicrobial activity. In the present work, the system RB–pHEMA is studied. RB was selected for two reasons: as stated, it is a propotypical $^1O_2$ photosensitizer and, owing to the formation of photoactive dimers, it may be efficient at even higher concentrations.

2. Experimental

RB (disodium salt, certified dye purity 93%) and pHEMA (20 kDa, density 1.15 g ml^{-1} at 25 °C) from Sigma-Aldrich, 1,3-diphenylisobenzofuran (DPBF) from Aldrich, and methylene blue (MB, puriss., ⩾95%) from Fluka were used as received. RB purity was checked spectroscopically and no signs of other absorbing or emitting species were found. Analytical grade ethanol (Biopack) and acetone (Dorwil) were used without further purification. Dichloromethane (DCM, Dorwil, analytical grade) was distilled before use. Water was deionized and 0.22 μm filtered in a Millipore-Q system. Microscope slides, cleaned by ultrasonication in acetone, ethanol and water (30 min in each solvent), were used as substrates for film formation. Thin films, prepared by spin coating using a spin coater WS-400B-6NPP/Lite (Laurell Technologies), were produced from ethanol solutions containing 30 mg ml^{-1} of pHEMA and different concentrations of RB, using a two-step acceleration program, reaching 2500 rpm after 30 s. Film thickness was determined by stylus profilometry using a Dektak 150 Profilometer (Veeco). Films with RB concentrations from 0.044 to 18 wt% were prepared. Dye molar concentrations, necessary for the calculation of absorption coefficients and modeling of self-quenching processes, were calculated as:

$$[RB] = (\rho \text{wt}\%/M)/(100 - \text{wt}\%), \quad (1)$$

where ρ is the density of the film and M is the molar mass of RB (1017.64 g mol^{-1}). As a working approximation, valid in the limit [RB] $\rightarrow$ 0, the density of the pure solid polymer (1150 g l^{-1}) was used, leading to the concentration range 0.0005 to *ca.* 0.25 M, corresponding at the highest concentration to an intermolecular distance of about 2 nm, *ca.* twice the molecular dimensions (see detailed calculations in the supplementary material, molecular dimensions and quenching radius).

Absorption spectra were recorded on a Shimadzu UV-3600 UV–vis-NIR spectrophotometer. A home-made sample holder was designed to allow absorbance determinations in different regions of the film in order to evaluate its optical quality. Absorption spectra were obtained against a film devoid of dye. Film surface quality was examined by optical microscopy using a Leica DMRX optical microscope.

Steady-state fluorescence spectra were recorded on a PTI model QM-4 spectrofluorometer. Fluorescence was measured using two different experimental setups: (A) back face detection with normal excitation and (B) back face detection with excitation incidence at an angle of 45° respect to the film surface. In setup A, a right-angle triangular quartz prism (PS911, Thorlabs N-BK7), positioned immediately after the film, was used to drive light emitted from the sample into the detection channel. In both cases home-made sample holders were used. Excitation wavelength was 520 nm in all cases and emission was detected in the

range 540–750 nm using a cut-off filter Schott OG 530 (0.2 cm thickness) in front of the monochromator in order to block excitation light, which was further reduced, particularly for setup A, by changing the position of the emission lens. Emission spectra were corrected for filter transmittance and detection responsivity with wavelength, the later provided by the manufacturer and checked in our laboratory. Fluorescence quantum yields were determined relative to the same dye (RB) in ethanol ($\Phi_F = 0.11$) [9], using a 50 μm pathlength quartz cuvette. It should be stressed that sample and reference are not geometrically equivalent. However, considering that pHEMA and glass have similar refractive indexes, according to our estimations the two extra quartz–ethanol interfaces in the reference lead to a negligible overestimation of Φ_F in the order of 0.5%. The reason for measuring fluorescence in two ways was to confirm the independence of results on the measuring setup. Fluorescence quantum yields were obtained from eight independent measurements in two different sets of samples. In order to evaluate the effect of humidity, fluorescence spectra were also obtained in dry and water-saturated argon atmospheres. For that purpose, a 1 cm quartz cuvette was adapted to hold a sample at 45° from excitation beam with back face detection allowing gas flow. All fluorescence measurements were performed at room temperature, (25 ± 2) °C.

The $^1O_2$ generation rate was measured using DPBF in distilled DCM as a chemical monitor [10, 11]. A halogen lamp (OSRAM HLX 64657FGX-24V, 250W) was used for illumination. A water filter was interposed between the lamp and the sample to block IR from the light source, while a glass filter Schott GG495 (0.2 cm thickness) was used to avoid self-sensitized photoperoxidation of the monitor due to direct excitation [12]. DPBF absorption was monitored at 415 nm. Φ_Δ values were determined using a 2 μM MB solution in DCM as reference ($\Phi_\Delta = 0.57$) [13]. The fraction of radiation absorbed by the film and the MB reference was calculated taking into account the emission spectrum of the excitation lamp and the filter transmittance. High initial DPBF concentrations (~9×10^{-5} M) were used in the experiments in order to ensure quantitative reaction of accessible $^1O_2$ with the chemical monitor, i.e. by working in conditions where the product between the quenching rate constant ($k_q = 1.6 \times 10^9\ M^{-1}\ s^{-1}$ in DCM) and DPBF concentration significantly exceeds the intrinsic deactivation of $^1O_2$ ($k_d = 1.6 \times 10^4\ s^{-1}$ in DCM), and consequently zero-order regime during the entire experiment [14]. Experiments were performed in a 1 cm quartz cuvette at room temperature on dry and humidified films immersed in the monitor solution under magnetic stirring. Humidification was produced by exposing the films to a water-saturated oxygen flow during 30 min. The DPBF absorbance was monitored in the solution below the film.

While absorption, fluorescence and $^1O_2$ generation studies were performed on thin films, laser flash-photolysis (LFP) measurements were performed on films of larger thickness due to sensitivity limitations. For that sake, *ca.* 2 μm thick films were prepared from the same solutions as thin films by deposition over a glass support and evaporation of the solvent at room temperature. Films were placed inside a 1 cm quartz cuvette in a LP920 LFP compartment (Edinburgh Instruments) at an angle of 45° with respect to both excitation and analysis beams. A Nd-YAG laser (Spectron, 8 ns @ 532 nm) and a horizontally driven Xe lamp (ORSAM XBO 150 W/1 OFR) were used for excitation and analysis, respectively. Two filters Schott KG5 (0.2 cm thickness) were used to eliminate IR from the laser excitation, while two filters Schott OG550 (0.2 cm thickness), one interposed between the lamp and the sample and the other between the sample and the detection system, were used to avoid photobleaching of the dye due to unwanted analysis light below 550 nm and to block scattered excitation light into the detector, respectively. Analysis light was detected using a photomultiplier tube (Hamamatsu R929), after passing through a computer controlled high throughput ¼ m f/2.5 monochromator (Sciencetech 9055F). To increase the signal-to-noise ratio, currently 64 traces were averaged. The analysis wavelength of triplet-triplet absorption was selected at 650 nm as a compromise between the signal-to-noise ratio, interference of the laser beam and dye photobleaching. The system was purged either with water-saturated oxygen or water-saturated argon, using always water-saturated gases to facilitate diffusion of O_2 in and out of the film [15].

In order to get insight into the self-quenching mechanisms, the dependence of Φ_F on dye concentration was fitted using a quenching radius model considering a 3D random distribution of dye molecules in the film and traps consisting of two or more dyes at distances within a quenching radius, r_Q. As a first approximation non-fluorescing, perfect traps were considered and energy migration and trapping efficiencies were calculated using LAF theory [16, 17], where r_Q was the fitting parameter. This model, called hereafter dark traps (DT) model due to the non-fluorescing nature of the traps, is similar to those used for fluorescence self-quenching studies in previous works [8, 18]. A second approximation, called bright dimeric traps (BDT) model, was applied. It uses the same formalism as the DT model for the calculation of energy trapping efficiencies but considers fluorescence emission from dye pairs within r_Q (BDT), higher-order (multimeric) traps remaining non-fluorescent. It is important to stress that the BDT model is a rough approximation because it considers only the energy transfer from monomers to traps, neglecting the possibility of energy transfer from dimeric bright traps to higher-order traps or back to the pool of monomers. For the BDT model, r_Q and the traps to monomer fluorescence quantum yields ratio, $\Phi_{F,trap}/\Phi_{F,monomer}$, were used as fitting parameters. For both

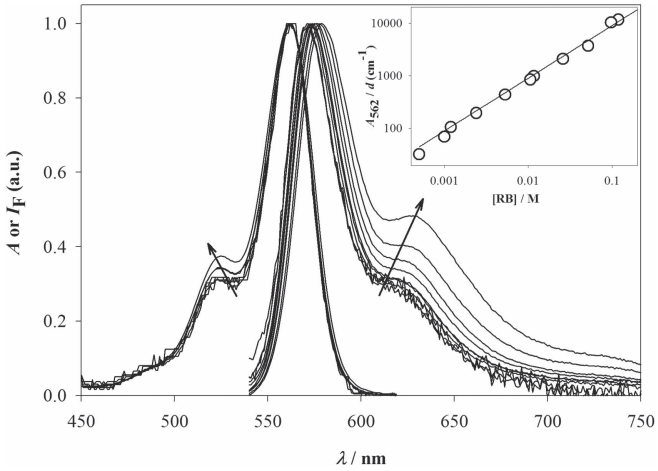

Figure 1. Normalized absorption spectra of RB-pHEMA films at RB concentrations higher than 0.01 M and normalized fluorescence spectra of RB-pHEMA films at dye concentrations from 0.001 M to *ca.* 0.25 M. Excitation wavelength 520 nm. Inset: absorbance at maximum (562 nm) per unit pathlength as a function of dye molar concentration.

models, the concentrations of monomers and traps were estimated considering Poisson statistics. Förster radii were calculated as $R_{0,M-M} = 33.3$ Å and $R_{0,M-T} = 37.3$ Å for monomer–monomer and monomer–trap energy transfer, respectively. The later parameter was calculated considering that the absorption coefficient of traps is twice the absorption coefficient of the monomeric dye. This is consistent with the traps arising from weakly interacting ground state dye molecules. An orientational parameter $\kappa^2 = 0.476$ (randomly distributed orientations fixed in time) and a refractive index $n = 1.51$ for pHEMA [19] were considered.

3. Results and discussion

Reproducible, (205 ± 24) nm thick films were obtained. No systematic effect of dye loading on film thickness was observed. Visual inspection through optical microscopy revealed a high surface homogeneity. Absorption spectra taken at different positions in the film showed negligible differences (see supplementary material, figure S1 is available online at stacks.iop.org/MAF/5/014010/mmedia). Normalized absorption spectra are shown in figure 1. For clarity, only the spectra at concentrations higher than 0.01 M are shown. Up to 0.05 M no spectral changes were observed, while above 0.05 M a slight increase in the shoulder absorbance around 520 nm is noticed, pointing to weak dye-to-dye interactions in the ground state motivated by crowding. The absorbance at maximum per unit pathlength, ($A_{max.}\ d^{-1}$), where d is the film thickness, follows a linear relationship with molar concentration, as shown in the inset. From these results, a value of (89 800 ± 2800) $M^{-1}\ cm^{-1}$ is obtained for the molar absorption coefficient at 562 nm, in the order of the value reported for RB at the absorption maximum in ethanol ($\varepsilon_{559nm} = 90\ 400\ M^{-1}\ cm^{-1}$) [9].

Normalized fluorescence spectra ($\lambda_{exc.} = 520$ nm) are also shown in figure 1. For simplicity, only spectra measured with setup A (back face detection with normal excitation, see experimental section) are shown in the figure. No significant differences were observed either in spectral shape or in relative intensity using setup B (see figure S2). Small spectral distortions due to emission reabsorption in the blue flank, noticed only at the highest concentrations, were corrected. For that sake, a correction considering inner filter effects in transmission geometry was applied [20]:

$$I_{f,corr}(\lambda) = I_{f,obs}(\lambda) \Big/ \left\{ \frac{A(\lambda_0)}{A(\lambda_0) - A(\lambda)} \cdot \frac{[10^{-A(\lambda)} - 10^{-A(\lambda_0)}]}{[1 - 10^{-A(\lambda_0)}]} \right\}, \quad (2)$$

where $I_{f,corr}(\lambda)$ and $I_{f,obs}(\lambda)$ are the corrected and experimentally observed fluorescence intensities, respectively, and A is the film absorbance measured at the excitation (λ_0) and emission (λ) wavelengths. Corrections were only significant for concentrations higher than 0.1 M and represented less than 8% of the experimentally observed fluorescence intensities in all cases. The red-shift and the increase of the shoulder around 620 nm on increasing concentration point to dye-to-dye interactions in the excited state at the highest concentrations.

Fluorescence quantum yields are shown in figure 2 as a function of dye concentration. No significant differences were found using either setup A or setup B (see experimental section and figure S3). Reproducibility was evaluated from eight independent measurements. Somewhat higher error bars at low concentrations (<0.005 M) are the result of uncertainties in the determination of the fraction of incident radiation absorbed at the excitation wavelength, due to the low absorbance of the samples. Experimental absorbances at the excitation wavelength for samples with [RB] <0.002 M were too low to be appreciated correctly and, therefore, they

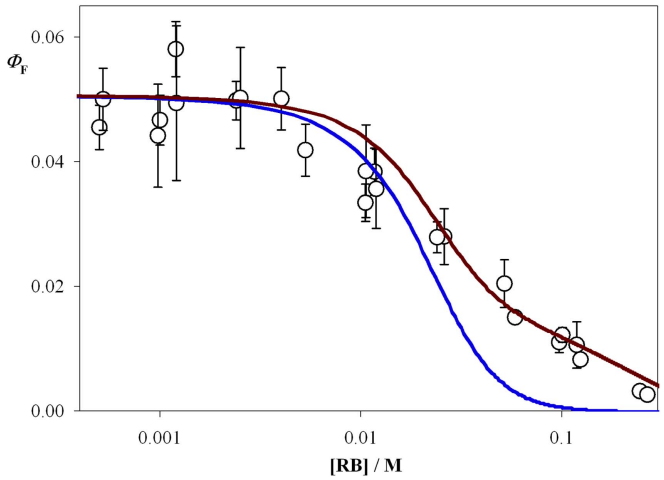

Figure 2. Fluorescence quantum yields of RB-pHEMA films (circles) on excitation at 520 nm as a function of dye concentration. Error bars correspond to one standard deviation from eight independent measurements using both measuring setups (see experimental section). Blue and red lines are theoretical fittings according to the quenching radius DT and BDT models, respectively (see text).

were calculated considering the linear dependence on dye concentration (figure 1 inset). It is clear from the figure that up to *ca.* 0.01 M fluorescence quantum yields are constant within the experimental error, leading to a value $\Phi_F = 0.05 \pm 0.01$ for the monomeric, isolated dye in the polymer. This value is intermediate between those reported for RB in ethanol solution, $\Phi_F = 0.11$ [9], and in water, $\Phi_F = 0.018$ [2]. The photophysical behavior of RB depends strongly on the environment. The strength of hydrogen-bonding in protic solvents has been recognized as an important factor affecting RB fluorescence lifetimes and quantum yields [2, 21]. According to Fleming *et al* the stabilization energies due to solute–solvent interactions of RB states in protic solvents lies in the order $\Delta E(T_1) < \Delta E(S_1) < \Delta E(S_0)$, leading to a blue-shift in absorption and a decrease in Φ_F on increasing solute–solvent interactions. The absorption maxima of RB in ethanol and water appear at 559 and 548 nm, respectively. The absorption maximum in pHEMA at 562 nm (see figure 1) points to a solvation interaction similar to that in ethanol. However, a Φ_F value lower than in ethanol is obtained, probably reflecting peculiarities of the solvation of the dye entrapped in the solid matrix.

The effect of humidity on fluorescence spectra and intensity was investigated. No significant changes were observed by comparing films dried with an argon flow and the as-prepared films in ambient conditions. On the other hand, a slight blue shift in fluorescence spectra (~1 nm) and a decrease in fluorescence intensity as high as 35% were obtained on humidification (see figure S4). As expected, fluorescence changes point to the dye sensing a water-like environment as the film is humidified. Irrespective of the fluorescence changes observed on humidification, the same trend, within the experimental error, was obtained for the concentration dependence of fluorescence quantum yields (see figure S5).

At RB concentrations from nearby 0.01 M self-quenching is clearly evidenced (see figure 2). Experimental results were fitted according to the DT model (see experimental section for calculation parameters and details), which considers non-emitting RB traps. The best fit was obtained with a quenching radius $r_Q = 1.5$ nm, in the order of molecular dimensions (see detailed calculations in the supplementary material, molecular dimensions and quenching radius). However, as shown in the figure, this model fails to reproduce quantum yields above *ca.* 0.03 M, predicting a more pronounced fall-off in Φ_F on increasing concentration. On the other hand, when the BDT model, considering emission from dimeric traps, is used, an excellent fit is obtained in the whole concentration range with $r_Q = 1.5$ nm and $\Phi_{F,trap}/\Phi_{F,monomer} = 0.35$, as shown also in figure 2. These results, together with the marked increase of the red-shoulder in the fluorescence spectra after correction of reabsorption on increasing concentration (see figure 1), point to the presence of bright traps, consistent with pairs of close-lying dye molecules interacting in the excited state. Our results are in line with previous evidence on dimer emission for RB in the polymeric constrained environment provided by cellulose microparticles [7]. In that case, a dimer to monomer fluorescence quantum yield ratio $\Phi_{F,dimer}/\Phi_{F,monomer} = 0.58$ was obtained, which is in the order of the ratio found in the present work. However, hypochromism in absorption spectra and slight changes in fluorescence spectra on increasing dye concentration were observed in that case. Further work on the photophysics of RB in a cellulose matrix in a larger concentration interval revealed that

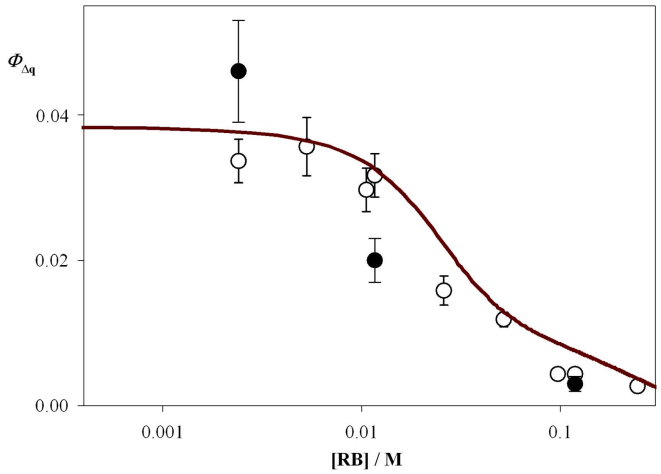

Figure 3. Quenchable singlet molecular oxygen quantum yield of dry (hollow circles) and humidified (filled circles) RB-pHEMA films as a function of dye concentration. The solid red line corresponds to the scaled BDT model fitting of fluorescence results (see text).

higher-order aggregates were dark and photochemically inactive [22].

Generation of $^1O_2$ in the films was evidenced by following the time-dependent decrease of a chemical monitor (DPBF) absorption in DCM solution at 415 nm when a film immersed in the solvent is irradiated within the absorption range of RB, as described in the experimental section. The slope in DPBF absorbance as a function of irradiation time is a measure of the rate of reaction between the monitor and $^1O_2$. In excess DPBF, a constant slope is expected, which is an estimate of the rate of $^1O_2$ production at the film surface (see below). Φ_Δ values were calculated in reference to MB in DCM ($\Phi_\Delta = 0.57$) [13]. No changes in DPBF absorption was observed in the dark. A slight constant decrease detected under illumination in the absence of the film, related to self-sensitized photoperoxidation of the monitor [12], was taken into account. No desorption of RB was spectroscopically evidenced. Φ_Δ values as a function of RB concentration are shown in figure 3.

From figure 3, it is seen that, up to RB 0.01 M, quantum yields are constant within the experimental error, $\Phi_{\Delta q} = 0.038 \pm 0.007$, where q stands for 'quenchable'. These low values reflect the fact that, on irradiation, only a fraction of $^1O_2$ is capable to diffuse out of the film in order to react with the chemical monitor. For that reason, experimentally obtained Φ_Δ values are strongly underestimated and refer to $^1O_2$ quenchable by DPBF. The quenchable fraction:

$$f = \frac{\Phi_{\Delta q}}{\Phi_\Delta} \tag{3}$$

can be estimated according to the Brownian motion equation in one-dimension, $x = (2Dt)^{1/2}$, where D is the diffusion coefficient of $^1O_2$. Taking into account that, from the $^1O_2$ molecules produced at a distance x from the film surface, one half diffuses in the wrong direction and, from the other half, only $\exp(-x^2/2D\tau)$ reaches the surface, where τ is the $^1O_2$ lifetime in pHEMA, for a film of thickness L:

$$f \approx \frac{1}{2} \cdot \frac{(2D\tau)^{1/2}}{L} \cdot \int_0^\infty \exp(-y^2)\,dy = \frac{(2\pi D\tau)^{1/2}}{4L}$$
$$\text{with} \quad y = \frac{x}{(2D\tau)^{1/2}}. \tag{4}$$

The model assumes that $^1O_2$ diffusing in the direction of the glass support, though reflected back, does not reach the free film surface. This approximation is valid for enough thick films (see below). A good guess of the diffusion coefficient can be made, considering hydrated (35 vol%) pHEMA crosslinked with tetraethylene glycol dimethacrylate, for which $D = 1.36 \times 10^{-7}$ cm^2 s^{-1} [15]. The $^1O_2$ lifetime in the polymer can be estimated as $\tau \approx 20\ \mu$s [23]. Considering these values, for $L \approx 200$ nm a quenchable fraction $f = 0.05$ is obtained. This means that only 5% of the $^1O_2$ generated in the films is able to reach the surface and react with the chemical monitor. Thinner films can, in principle, be used to increase this factor, but the uncertainty in film absorbance would be too high for a quantitative evaluation of Φ_Δ. Moreover, according to these calculations, the amount of $^1O_2$ reaching the surface would be independent of film thickness, provided it is higher than $(2D\tau)^{1/2}$, a distance amounting a few tens of nanometers. This ensures in turn that reflected $^1O_2$ decays within the film, not reaching the surface. The overall value of Φ_Δ can then be estimated at low concentrations as $\Phi_\Delta = \Phi_{\Delta q}/f = 0.76 \pm 0.14$. Within this rather large uncertainty, this value is similar to those reported for RB in ethanol (0.68) [24], methanol (0.80 ± 0.02) and water (0.76 ± 0.02) [25].

As shown in figure 3, at concentrations higher than *ca.* 0.01 M, a marked decrease of $\Phi_{\Delta q}$ is observed on increasing concentration. For comparison, the BDT model fitting of fluorescence results, scaled to fit the quantum yield at low concentrations, is also shown in the figure. Almost the same trend as Φ_F is observed for $\Phi_{\Delta q}$ on increasing dye concentration. At first glance,

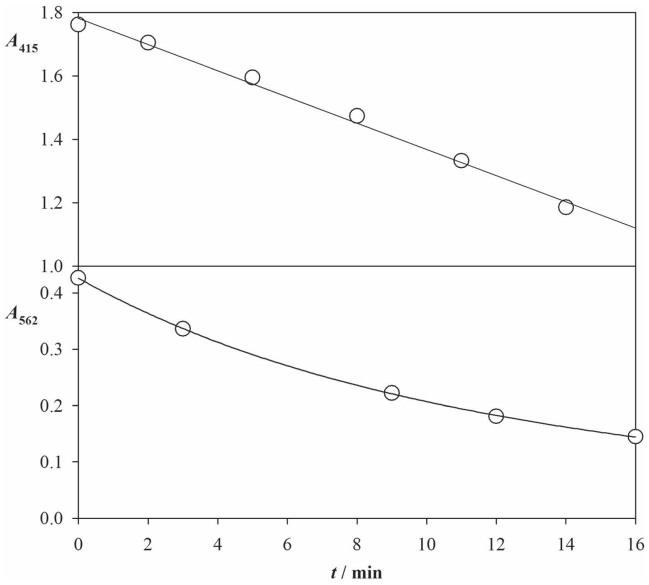

Figure 4. DPBF absorption (upper circles) and RB absorption at maximum (lower circles) as a function of irradiation time in separate singlet molecular oxygen experiments for a 0.24 M RB pHEMA film. Solid lines are linear and exponential fittings for DPBF and RB, respectively.

results would suggest that fluorescence and $^1O_2$ generation are quenched to a similar extent as concentration increases. This point will be addressed below on discussing figure 6.

Humidity induces swelling of the polymer matrix, increasing the oxygen diffusion coefficient [15]. For that reason, increased $\Phi_{\Delta q}$ values were expected for humidified films, as previously observed for PhB in pHEMA [8]. However, a few experiments conducted with humidified, oxygen-saturated samples (see figure 3) show no neat effect of humidity on $\Phi_{\Delta q}$. More experiments, together with detailed studies on oxygen diffusion, lifetime and triplet quantum yields in RB-pHEMA films as a function of water content, which are out of the scope of the present work, are needed to certify this behavior and to reach a satisfactory explanation.

As mentioned above, the $^1O_2$ generation rate in the films was determined by measuring the decrease of DPBF absorbance as a function of irradiation time, in the zero-order kinetic regime, i.e. at constant reaction rate (constant slope). However, examination of the films before and after polychromatic irradiation showed in all cases marked photobleaching. The course of the absorbances of DBPF and RB, obtained in separate but otherwise similar experiments, are shown in figure 4. The figure shows that, while zero-order kinetic is followed by DPBF during the first 15 min, dye photobleaching reaches more than 60% within the same time interval. It is noteworthy that following dye photodegradation required the adaptation of the $^1O_2$ measuring setup in order to follow the absorption of the film within the irradiated area. Therefore, the analysis of photodegradation was performed on a duplicate film, maintaining all the other conditions used for DPBF analysis, which involves absorbance measurements in the solution below the film.

Considering that DPBF senses only $^1O_2$ reaching the film surface, results shown in the figure may be explained only if dye photobleaching takes place mainly in the film bulk. RB photobleaching may involve reactions of the dye triplet with close-lying ground state dye molecules, with the solid matrix and with molecular oxygen or reaction of ground state RB with $^1O_2$ [26–29]. Most probably, the reaction of RB with photogenerated $^1O_2$ is the prevalent mechanism. On the other hand, $^1O_2$ generated at or near the film surface reacts mainly with DPBF. This means that the chemical monitor may be acting as a protection against dye photobleaching. In that case, even when massive photobleaching is evidenced through the decrease of RB absorption, a negligible decrease may be expected near the surface. It is important to stress that dissolved oxygen consumption is negligible during these experiments (<1.5% in all cases). Though strong dye photobleaching is observed under irradiation in the conditions of $^1O_2$ experiments, normal manipulation and storage and exposition to laboratory illumination yielded less than 35% decomposition after 2 months.

LFP was used to evidence triplet state formation of RB in the films and its quenching in the presence of molecular oxygen. As triplet–triplet absorption was not detected in thin films, films of *ca.* 2 μm thickness were used in these experiments (see experimental section). Transient decays of a RB-pHEMA film containing 0.052 M RB are shown in figure 5. After purging with humidified argon, monoexponential decay is obtained, with a triplet lifetime of (153 $\pm$ 3) μs. This value is

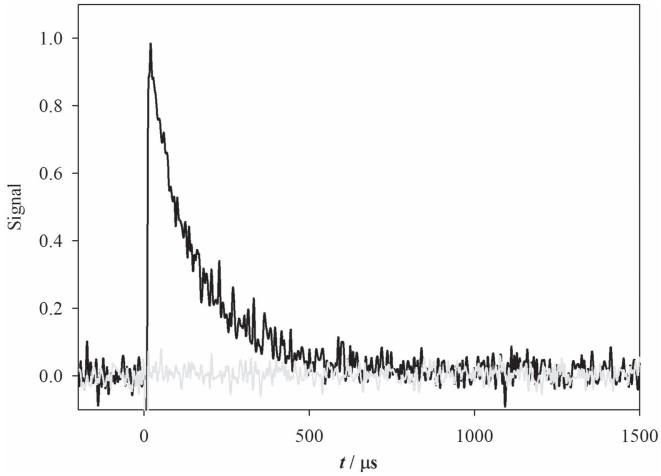

Figure 5. Triplet–triplet absorption decay of a 0.052 M RB-pHEMA thick film (2 μm thickness) measured at 650 nm after purging with humidified argon (black line) and absence of signal after purging with humidified oxygen (gray line).

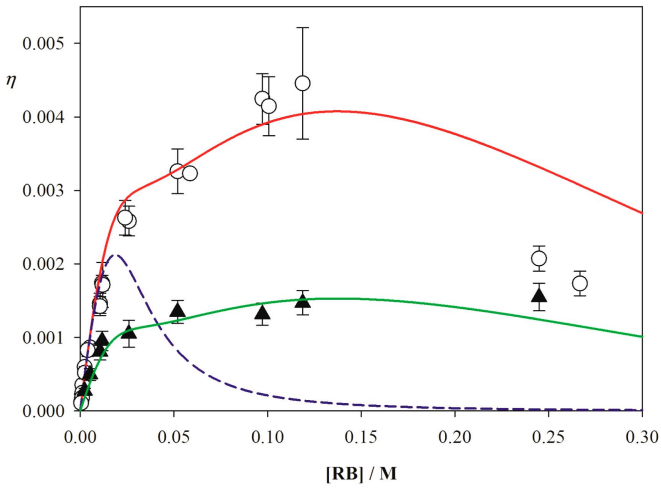

Figure 6. Experimental efficiencies for fluorescence emission (circles) and $^1O_2$ generation (triangles) excited at 562 nm as a function of dye concentration. The solid red and dashed blue lines are fluorescence fittings according to the BDT and DT models, respectively. The solid green line is the red line scaled down to fit $^1O_2$ generation data (see text).

similar to those reported in ethanol, (90 $\pm$ 4) μs [30], and water, 150 μs [31]. After purging with humidified oxygen, the signal vanishes, as expected for quantitative triplet quenching in the presence of oxygen. The effect can be reversed, recovering the signal by purging again with humidified argon.

The efficiencies of fluorescence emission and $^1O_2$ generation at the film surface, η_F and $\eta_{\Delta q}$, can be estimated as:

$$\eta = \Phi(1 - 10^{-A(\lambda_0)}) \approx 2.303\Phi\varepsilon_{\lambda_0}[\mathrm{RB}]L, \qquad (5)$$

where Φ is Φ_F or $\Phi_{\Delta q}$ and $A(\lambda_0)$ and $\varepsilon_{\lambda 0}$ are the sample absorbance and the absorption coefficient of RB at the excitation wavelength, λ_0. These efficiencies have the meaning of a rate divided by the incident photon flow. Fluorescence results for excitation at the RB absorption maximum (λ = 562 nm) are shown in figure 6 together with theoretical calculations according to the BDT and DT models. Theoretical Φ_F values were obtained from figure 2 for the corresponding model and absorption factors were calculated for a film thickness of 200 nm using the experimental value of $\varepsilon_{562\ \mathrm{nm}}$. The BDT model fits properly the fluorescence data. The large deviation found at the highest concentrations, magnified by the way in which results are plotted (compare with figure 2), is probably due to underestimated measurement errors at extremely low quantum yield values. On the other hand, the DT model does not fit experimental data after [RB] = 0.01 M, showing that dimer emission plays a relevant role in the whole region where self-quenching takes place. The greatest fluorescence efficiency is around 0.004, that is, 0.4% of the incident photons at 562 nm result in fluorescence, and is obtained for RB concentrations about 0.15 M (~10 wt%). The maximum efficiency for PhB in pHEMA films was found at concentrations around 0.03 M [8], in the order of the value predicted by the DT model in this work. The presence of photoactive dimeric traps in RB-pHEMA

films is responsible for the increase in the concentration at which efficiency reaches its maximum.

The $^1O_2$ generation efficiency is also shown in figure 6. In addition, the figure shows the result according to the BDT model scaled down to fit $^1O_2$ generation data at intermediate concentrations. The scale factor is different to that used to fit $\Phi_{\Delta q}$ in figure 3. This fact may be explained assuming that Φ_Δ/Φ_F is different for the monomer and dimeric traps. The maximum found for the $^1O_2$ generation efficiency is 0.0015, meaning that 0.15% of the incident photons at 562 nm result in $^1O_2$ generation at the film surface. This value seems rather low. It arises from the small absorbance of the nanometric film together with the low fraction of photogenerated $^1O_2$ which can be quenched at its surface. However, taking into account the high absorption coefficient of RB, the high overall Φ_Δ value and the magnitudes of D and τ, which are standard values for various polymers, this efficiency could hardly be exceeded by any other heterogeneous photosensitizer and would be independent of L for film thicknesses not lower than a few tens of nanometers but enough low to ensure linearity between the absorption factor and A_λ:

$$\eta_{\Delta_q} = 2.303 f \Phi_\Delta \varepsilon_{\lambda 0} [\mathrm{RB}] L = 2.303 \frac{(2\pi D\tau)^{1/2}}{4} \Phi_\Delta \varepsilon_{\lambda 0} [\mathrm{RB}], \quad (6)$$

where Φ_Δ is the actual singlet molecular oxygen quantum yield. The relevant factors in selecting a dye-polymer couple are Φ_Δ for the monomeric dye, a low quenching radius and a high absorption coefficient. The occurrence of bright traps, together with increasing somewhat the efficiency, has mainly the effect of increasing the dye concentration at which its maximum is attained.

4. Conclusions

Applications of dye loaded polymer films were listed in [8]. Those like optical mass storage and photosensitization under low illumination conditions require high dye concentrations, at which the distance among chromophores becomes rather small, in the order of molecular dimensions. In this case, dye-to-dye interactions take place, leading to enhanced radiationless deactivation.

The photophysical properties of RB included in pHEMA at low concentrations are similar to those found in dilute water and ethanol solution. On increasing the concentration in the polymer, molecular crowding leads to the occurrence of weak interactions between close-lying dye molecules in their ground state. In general, upon excitation through light absorption or energy transfer, molecular pairs undergo radiationless deactivation leading to energy trapping. However, though self-quenching takes place to some extent, in the case of RB dimeric traps are imperfect: they are able to fluoresce and build up $^1O_2$ in the presence of molecular oxygen. At even higher concentrations, dark oligomers are formed. As a consequence, Φ_F and Φ_Δ decrease with concentration to a lesser extent than in cases where perfect DT are formed [8].

Quantum yields can be modeled assuming random distribution of dye molecules (statistical trapping) under the formalism of LAF theory. As a consequence of formation of BDT, the efficiency of fluorescence emission and $^1O_2$ generation reach their maxima at [RB] $\approx$ 0.15 M. Thus, even for systems with randomly distributed dyes, very high concentrations can be used for the design of dye-loaded photoactive polymeric materials. The quenching radius is calculated as $r_Q = 1.5$ nm, which represents the minimum distance at which dye molecules can be located in order to prevent self-quenching. This radius constitutes an important parameter for the design of systems with ordered arrays of dyes. Oxygen diffusion determines the maximum effective thickness for the development of $^1O_2$ generating coatings. Φ_F values, whose measurement is very easy and more accurate than Φ_Δ, is a key method for the photophysical characterization of thin films.

Acknowledgments

This work has been supported by the Universidad de Buenos Aires (UBACyT 20020130100166BA), the Consejo Nacional de Investigaciones Científicas y Técnicas (CONICET PIP 112-201101-00467) and the Agencia Nacional de Promoción Científica y Tecnológica (ANPCyT PICT 2012-2357 and 2014-2153). The funders had no role in study design, data collection and analysis, decision to publish, or preparation of the manuscript. HBR and ESR are staff members of CONICET. The authors have declared that no conflicting interests exist.

Author contributions

The manuscript was written through contributions of all authors. All authors have given approval to the final version of the manuscript.

Notes

The authors declare no competing financial interest.

References

[1] Kochevar I E and Redmond R W 2000 Photosensitized production of singlet oxygen *Methods Enzimol.* **319** 20–8
[2] Fleming G R, Knight A W E, Morris J M, Morrison R J S and Robinson G W 1977 Picosecond fluorescence studies of xanthene dyes *J. Am. Chem. Soc.* **99** 4306–11
[3] Tomasini E P, Braslavsky S E and San Román E 2012 Triplet quantum yields in light-scattering powder samples measured

by laser-induced optoacoustic spectroscopy (LIOAS) *Photochem. Photobiol. Sci.* **11** 1010–7
[4] Neckers D C 1985 Heterogeneous sensitizers based on merrifield copolymer beads *Reactive Polym.* **3** 277–98
[5] Lopez S G, Crovetto L, Alvarez-Pez J M, Talavera E M and San Román E 2014 Fluorescence enhancement of a fluorescein derivative upon adsorption on cellulose *Photochem. Photobiol. Sci.* **13** 1311–20
[6] Reisch A and Klymchenko A S 2016 Fluorescent polymer nanoparticles based on dyes: seeking brighter tools for bioimaging *Small* **12** 1968–92
[7] Rodríguez H B, Lagorio M G and San Roman E 2004 Rose bengal adsorbed on microgranular cellulose: evidence on fluorescent dimmers *Photochem. Photobiol. Sci.* **3** 674–80
[8] Litman Y, Rodríguez H B and San Román E 2016 Tuning the concentration of dye loaded polymer films for maximum photosensitization efficiency: phloxine B in poly(2-hydroxyethyl methacrylate) *Photochem. Photobiol. Sci.* **15** 80–5
[9] Seybold P G, Gouterman M and Callis J 1969 Calorimetric, photometric and lifetime determinations of fluorescence yields of fluorescein dyes *Photochem. Photobiol.* **9** 229–42
[10] Figueiredo T L C, Johnstone R A W, SantAna Sørensen A M P, Burget D and Jacques P 1999 Determination of fluorescence yields, singlet lifetimes and singlet oxygen yields of water-insoluble porphyrins and metalloporphyrins in organic solvents and in aqueous media *Photochem. Photobiol.* **69** 517–28
[11] Mirenda M, Strassert C A, Dicelio L E and San Roman E 2010 Dye-polyelectrolyte layer-by-layer self-assembled materials: molecular aggregation, structural stability, and singlet oxygen photogeneration *ACS Appl. Mater. Interfaces* **2** 1556–60
[12] Nowakowska M 1984 Solvent effect on the quantum yield of the self-sensitized photoperoxidation of 1,3-diphenilisobenzofuran *J. Chem. Soc. Faraday Trans.* **1** 2119–26
[13] Usui Y 1973 Determination of quantum yield of singlet oxygen formation by photosensitization *Chem. Lett.* **2** 743–4
[14] Usui Y, Tsukada M and Nakamura H 1978 Kinetic studies of photosensitized oxygenation by singlet oxygen in aqueous micellar solutions *Bull. Chem. Soc. Japan* **51** 379–84
[15] Parker J W and Cox M E 1988 Mass transfer of oxygen in poly (2-hydroxyethyl methacrylate) *J. Polym. Sci.* A **26** 1179–88
[16] Loring R F, Andersen H C and Fayer M D 1982 Electronic excited state transport and trapping in solution *J. Chem. Phys.* **76** 2015–27
[17] Kulak L and Bojarski C 1995 Forward and reverse electronic energy transport and trapping in solution: II. Numerical results and Monte Carlo simulations *Chem. Phys.* **191** 67–86
[18] Lopez S G, Worringer G, Rodríguez H B and San Román E 2010 Trapping of Rhodamine 6G excitation energy on cellulose microparticles *Phys. Chem. Chem. Phys.* **12** 2246–53
[19] De Girolamo Del Mauro A, Grimaldi A I, La Ferrara V, Massera E, Miglietta M L, Polichetti T and Di Francia G 2009 A simple optical model for the swelling evaluation in polymer nanocomposites *J. Sens.* **2009** 703206
[20] Krimer N I, Rodrigues D, Rodríguez H B and Mirenda M 2017 Steady-state fluorescence of highly absorbing samples in transmission geometry: a simplified quantitative approach considering reabsorption events *Anal. Chem.* **89** 640–7
[21] Kramer L E and Spears K G 1978 Hydrogen bond strengths from solvent-dependent lifetimes of rose bengal dye *J. Am. Chem. Soc.* **100** 221–7
[22] Litman Y, Voss M G, Rodríguez H B and San Román E 2014 Effect of concentration on the formation of rose bengal triplet state on microcrystalline cellulose: a combined laser-induced optoacoustic spectroscopy, diffuse reflectance flash photolysis, and luminescence study *J. Phys. Chem.* A **118** 10531–7
[23] Rabek J F 1996 *Photodegradation of Polymers: Physical Characteristics and Applications.* (Berlin: Springer) p 87
[24] Gottschalk P, Paczkowski J and Neckers D C 1986 Factors influencing the quantum yields for rose bengal formation of singlet oxygen *J. Photochem.* **35** 277–81
[25] Wilkinson F, Helman W P and Ross A B 1993 Quantum yields for the photosensitized formation of the lowest electronically excited singlet state of molecular oxygen in solution *J. Phys. Chem. Ref. Data* **22** 113–262
[26] Talhavini M and Atvars T D Z 1999 Photostability of xanthene molecules trapped in poly(vinyl alcohol) (PVA) matrices *J. Photochem. Photobiol.* A **120** 141–9
[27] Kasche V and Liindqvist L 1964 Reactions between the triplet state of fluorescein and oxygen *J. Phys. Chem.* **68** 817–23
[28] Song L, Varma C A G, Verhoeven A J W and Tanke H J 1996 Influence of the triplet excited state on the photobleaching kinetics of fluorescein in microscopy *Biophys. Chem.* **70** 2959–68
[29] Roncel M, Navarro J A and de la Rosa M A 1996 Hydrogen peroxide photoproduction sensitized with rose bengal with semicarbazide as the electron source *J. Photochem. Photobiol.* A **45** 341–53
[30] Kamat P V and Fox M A 1984 Photophysics and photochemistry of xanthene dyes in polymer solutions and films *J. Phys. Chem.* **88** 2297–302
[31] Lee P C C and Rodgers M A J 1987 Laser flash photokinetic studies of rose bengal sensitized photodynamic interactions of nucleotides and DNA *Photochem. Photobiol.* **45** 79–86